Fundamental Study of Synthesis of Carbon and Boron Nitride Nanostructures in Atmospheric Pressure Arc Discharges

Igor Kaganovich for the Project Team

Princeton Plasma Physics Laboratory
MAE, Chemistry, CBE, EE Departments of Princeton University
Stony Brook University
George Washington University
Case Western Reserve University

EPS meeting, Prague, June 3, 2018

U.S. DEPARTMENT OF ENERGY | Office of Science

PPPL PRINCETON PLASMA PHYSICS LABORATORY

PRINCETON UNIVERSITY

Outline

Project research objectives, scope, highlights

Project accomplishments and major scientific results:

- **Simulations of arc structure and nanoparticle nucleation and growth**
- **Unique in situ diagnostics of plasma–based synthesis.**
- **Atomistic simulations of key processes of nanotube growth**
- **Nonstationary processes in arcs**

Summary

Plasma Science Studies of Nanomaterial Synthesis

- **Goal: Uncover long standing puzzle how nanotube grow for plasma synthesis of carbon and boron nitride nanostructures, by identification of exact conditions when nanotubes grow.**
- **Devices: Plasma arc and DC or RF plasma torches, laser-ablation.**
- **Approach: Perform detailed characterization of plasma and nanoparticles parameters using laser diagnostics; develop integrated and validated models comprised of numerical tools capable of simulating nucleation of nano-material growth and particle transport and plasma properties.**

Images of boron nitride nanotubes and boron catalyst particles.

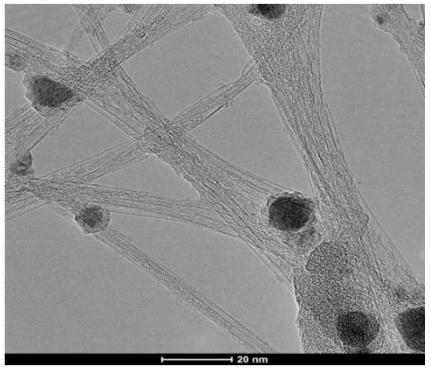

Arc as a versatile method of nanomaterial synthesis

- Many nanostructures were synthesized at different arc conditions: C60, MWCNT, SWNT, graphene flakes, nanofibers
- A graphite anode provides carbon feedstock to produce plasma and nanomaterials.

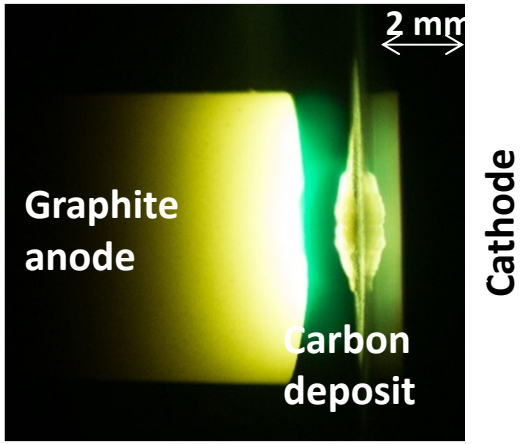

1-2 kW input power
Helium buffer gas
Atmospheric pressure
10 A/cm^2, 10's of Volts

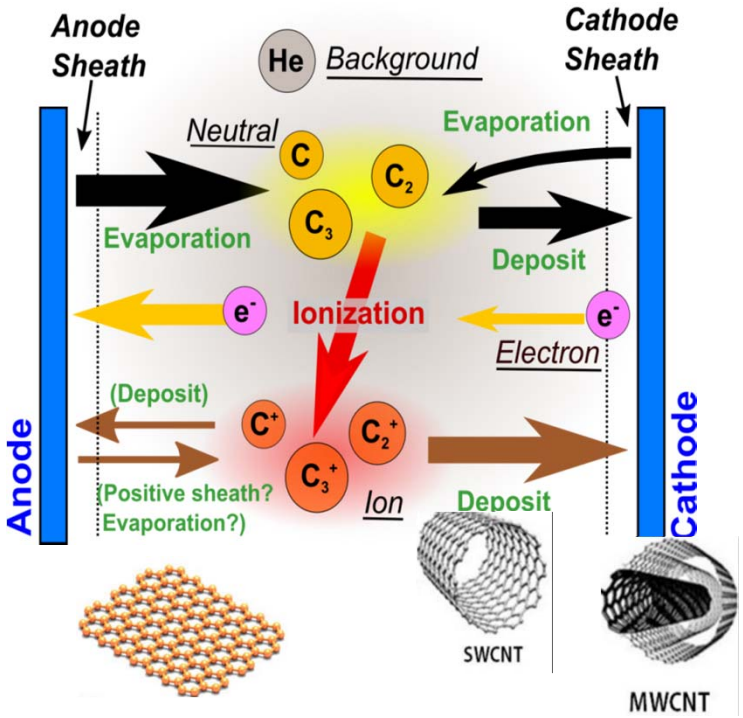

Fundamental Studies of Synthesis of Nanomaterials: A joint challenge for plasma and materials sciences

A central objective of the research is to understand the synergistic roles of plasma and materials processes in arc synthesis of Carbon and Boron Nitride (BN) nanotubes (CNTs, BNNTs)

- **Characterization of the plasma**
- **In-situ laser diagnostics of nanoparticles**
- **Ex-situ diagnostics of nanoparticles**
- **Development, validation, and integration of codes for multi-scale modeling of plasma nanosynthesis**

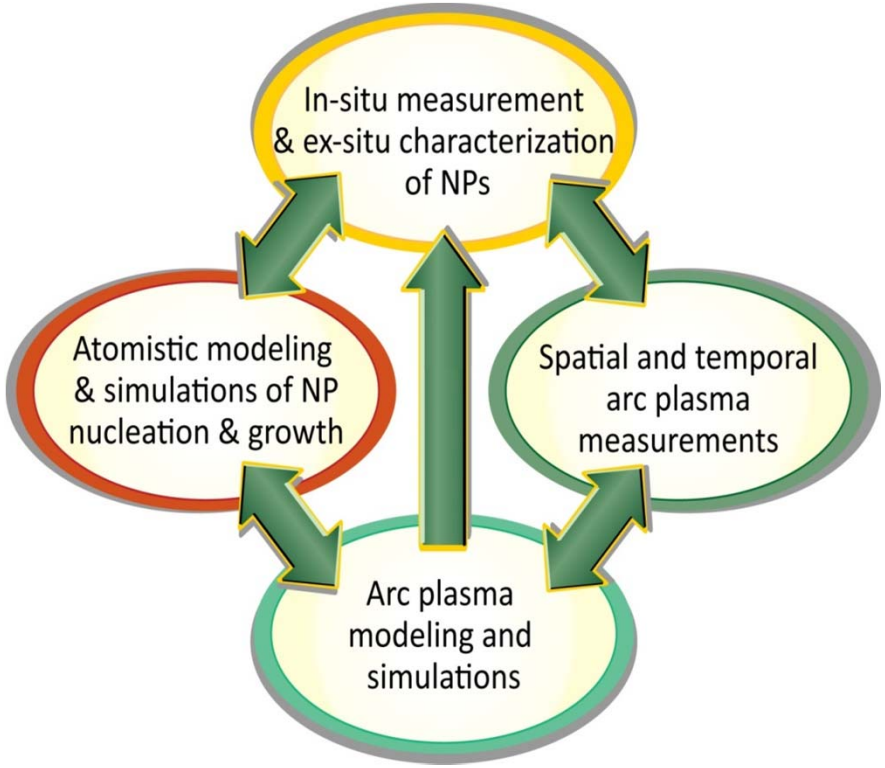

Laboratory for Plasma Nanosynthesis **consists of PPPL experts of in plasma science with the materials scientists of Princeton University and other institutions.**

materials diagnostics.

U.S. DEPARTMENT OF ENERGY | Office of Science

PPPL PRINCETON PLASMA PHYSICS LABORATORY

PRINCETON UNIVERSITY

THE GEORGE WASHINGTON UNIVERSITY WASHINGTON DC

Stony Brook University

CASE WESTERN RESERVE UNIVERSITY EST. 1826 think beyond the possible


Yevgeny Raitses (PPPL)


Igor Kaganovich (PPPL)


Brentley Stratton (PPPL)


Roberto Car (Princeton Univ.)


Mikhail Shneider (Princeton Univ.)


Rachel Selinsky (PPPL)


Alexandros Gerakis (PPPL)


Sophia Gershman (PPPL)


Kentaro Hara (PPPL)


Andrei Khodak (PPPL)


Michael Keidar (George Washington Univ.)


Alexnader Khrabry (PPPL)


Bruce Koel (Princeton Univ.)


Predrag Krstic (Stony Brook Univ.)


Longtao Han (Stony Brook Univ.)


James Mitrani (PPPL)


Valerian Nemchinsky (Keisa Univ.)


Angie Capece


Biswajit Santra (Princeton Univ.)


Mohan Sankaran (Case Western Reserve Univ.)


Vladislav Vekselman (PPPL)


Yao-Wen Yeh (PPPL)


Shurik Yatom (PPPL)

Computational tools used for simulations of arc plasma and nucleation and growth of nanostructures

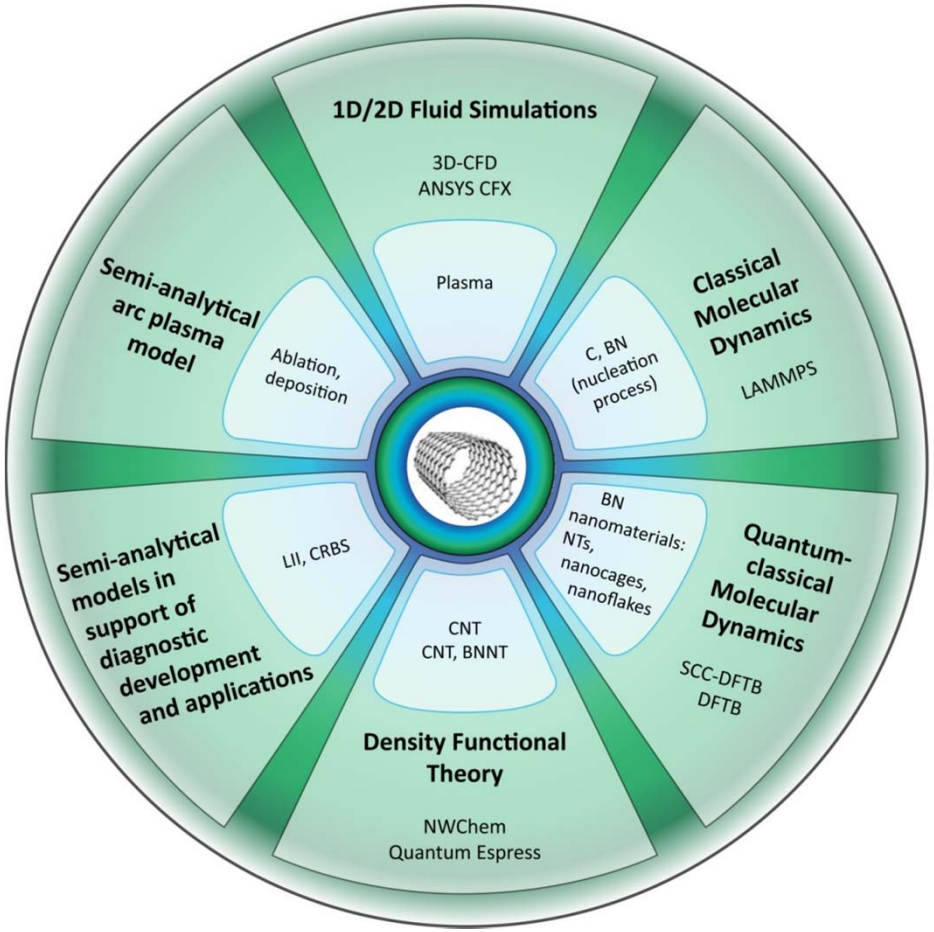

Outline

- **Simulations of arc structure and nanoparticle nucleation and growth**

Proposed hypothesis of carbon arc nanosynthesis

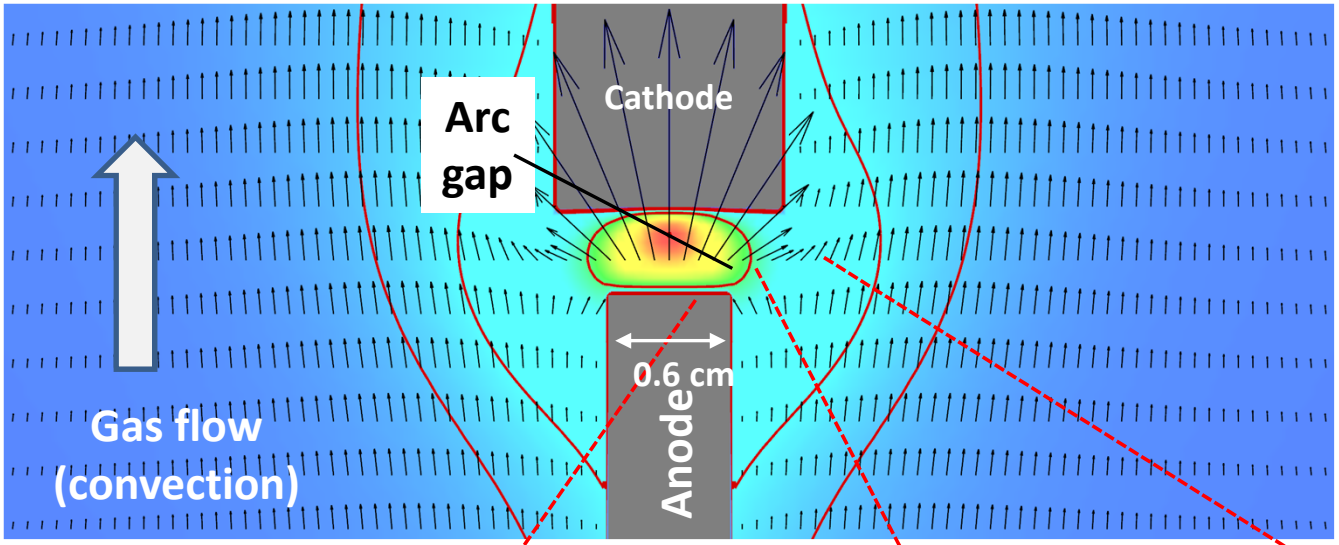

Vapor–liquid–solid

Gas temperature, K

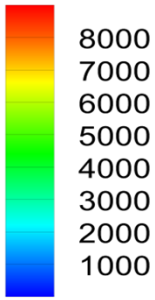

T = 4000 K

Evaporation, Dissociation

$C \approx 10^{17} – 10^{18}$ cm^{-3}

$He \approx 3 \cdot 10^{17}$ cm^{-3}

$C^{+} \approx 10^{14} – 3 \cdot 10^{16}$ cm^{-3}

T = 3000 K

Clusters, nucleation

$C \approx 10^{15} – 10^{16}$ cm^{-3}

$He \approx 3 \cdot 10^{18}$ cm^{-3}

$C^{+} \sim 10^{12}$ cm^{-3}

T = 2000 K

Growth, bundling

$C \approx 10^{14} – 10^{15}$ cm^{-3}

$He > 3 \cdot 10^{18}$ cm^{-3}

$C^{+} \approx 10^{10}$ cm^{-3}

Governing plasma equations

2D-3D model, C-He plasma

Momentum equation: $\nabla \cdot (\rho \vec{v}\vec{v}) = -\nabla p + \nabla \cdot (\mu \nabla \vec{v}) + \rho \vec{g}$

Continuity equation: $\nabla \cdot (\rho \vec{v}) = 0$

Neutral transport equation: $\nabla \cdot (\rho c_C \vec{v}) = \nabla (D \nabla (\rho c_C)) - S_i$

Ions transport equation: $\nabla \cdot (n_i \vec{v}) = \nabla (D_a \nabla n_i + D_{th\,diff} \nabla T + D_{th\,diff,e} \nabla T_e + j_e \gamma_{e,i}) + S_i, \quad S_i = \alpha n_e n_{C,Ar} - \beta n_e^3$

Transport of electrons: $\vec{E} = \nabla V = -\frac{k}{e}(1 + C_e^{(e)}) \nabla T_e - \frac{k}{e} T_e \nabla \ln n_e + \frac{\vec{j}_e}{\sigma}$

Equation of state: $p = (n_{neutrals} + n_i) kT + n_e k T_e$

Energy balance of electrons: $\nabla \cdot \left((2.5 + A_e) k T_e \frac{\vec{j}_e}{e} \right) = \nabla \cdot (\lambda_e \nabla T_e) - S_i E_i - Q^{electrons-heavy} - Q^{rad} + \vec{j} \cdot \vec{E}$

Energy balance of heavy particles: $\nabla \cdot (\rho \varepsilon \vec{v}) = \nabla \cdot (\lambda \nabla (T)) + Q^{electrons-heavy} + \vec{j}_i \cdot \vec{E}$

Quasi neutrality: $n_e = n_i$

$Q^{electrons-heavy}, \sigma, \lambda_e$ *are functions of* $(T_e, T, n_e, n_a, Q_{e,i}, Q_{e,a})$

2D setup: boundary and interfacial conditions

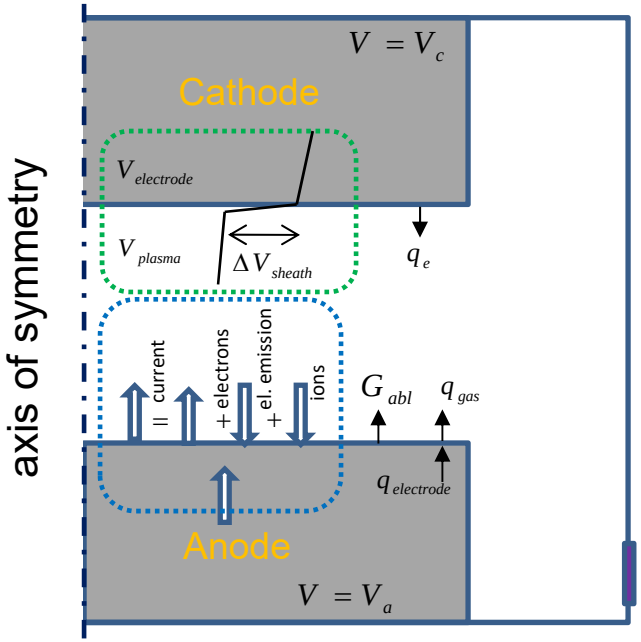

Plasma-electrode interfaces:

Ablation-deposition:

$$G_{abl} = \left(p_{satur,k}(T) - p_k\right)\sqrt{M_c/(2\pi RT)} \qquad p_k = n_k kT$$

Electric current and potential:

$$V_{solid} = V_{plasma} + \Delta V_{sh}$$

$$j_{n,plasma} = j_e^{emission} - j_e^{plasma\ \ to\ electrode} + j_i = f(\Delta V_{sh}, T, T_e, n_e)$$

Heat fluxes include processes: ablation and deposition, emission, radiation, sheath, work function, ionization.

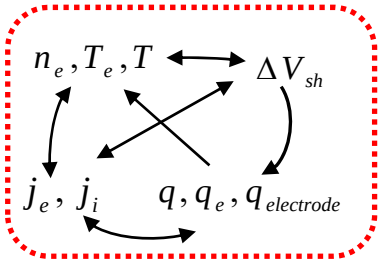

Very nonlinear self-consisted model with many parameters coupled at electrodes:

The current density is non-uniform at the electrode surfaces

Benchmarking of the model, 1D simulations

Argon arc, near-cathode layer: nonequilibrium region, effects of boundary conditions

our code, simulations by N. Almeida *et al.* A. Khrabry *et al*, Phys. Plasmas (2018)

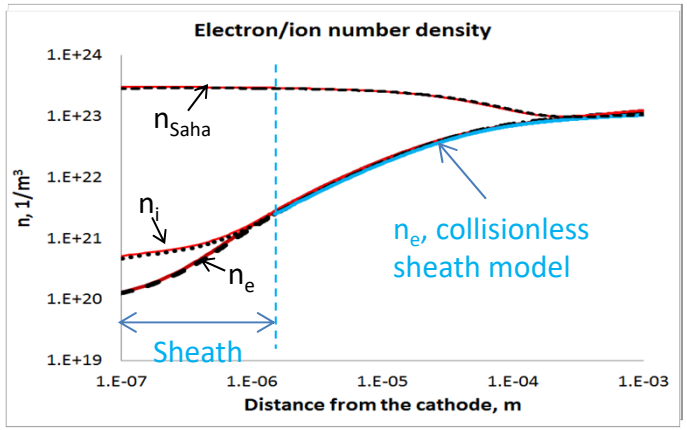

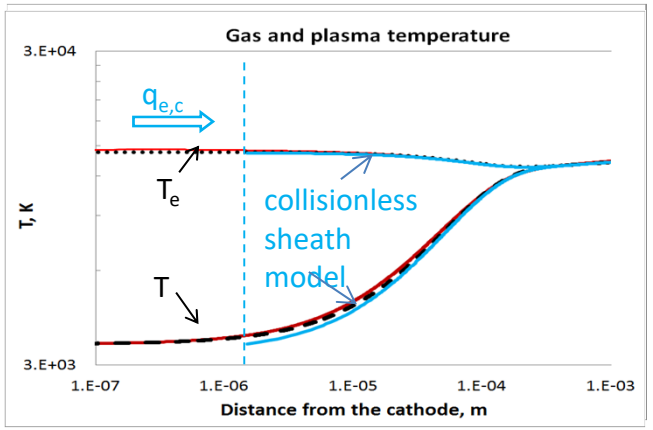

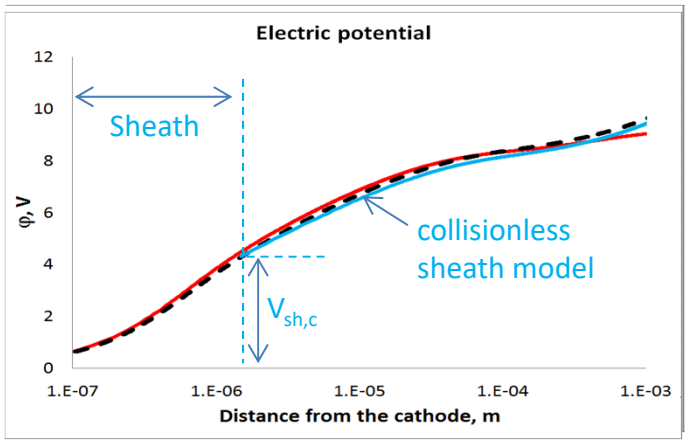

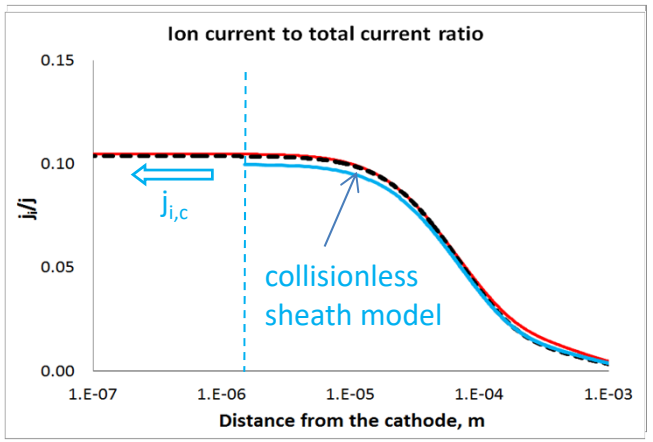

P = 1 atm

j = 5·10⁶ A/m²

$T_{cathode}$ = 3500K

Collisionless sheath model:

$$j = j_{e,c}^{p} + j_{e,c}^{emiss} + j_{i,c}$$

$$j_{i,c} = q_e n_i \sqrt{\frac{k(T_e + T)}{m_a}}$$

$$j_{e,c}^{p} = q_e n_e \frac{1}{4}\sqrt{\frac{kT_e}{m_e}} \cdot e^{-\frac{V_{sh,c}}{kT_e}}$$

$$q_{e,c} = j_{e,c}^{emiss}\left(V_{sh,c} + 2.5T_c\right) - j_{e,c}^{p}\left(V_{sh,c} + 2.5T_e\right)$$

Self-consistent current density profile

Simulations:

Electric current streamlines:

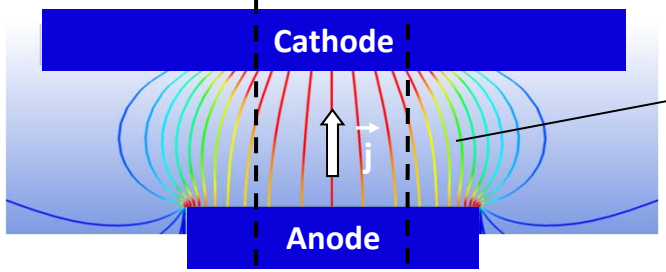

Electric potential profile:

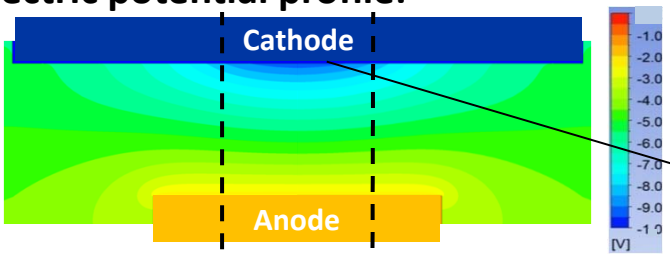

Non-uniform potential profile along the cathode.

Experiments with a segmented cathode:

Y.-W. Yeh et.al., Carbon 2016

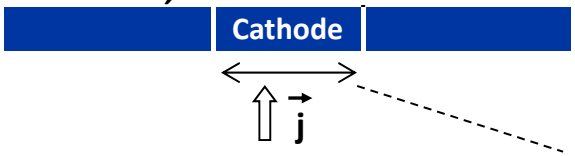

2 radial segments, central segment d=3.2mm, 95% of current

Simulations: 75% of current flows through 3.2mm segment

V. Vekselman, et al PSST 2017

Arc channel

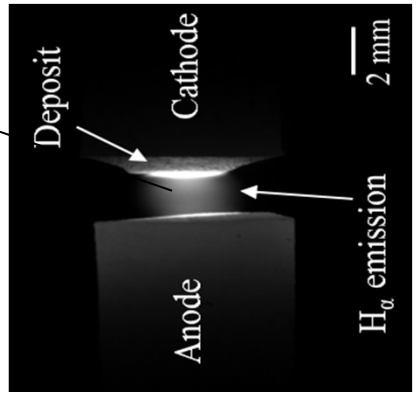

Middle plane plasma density profile:

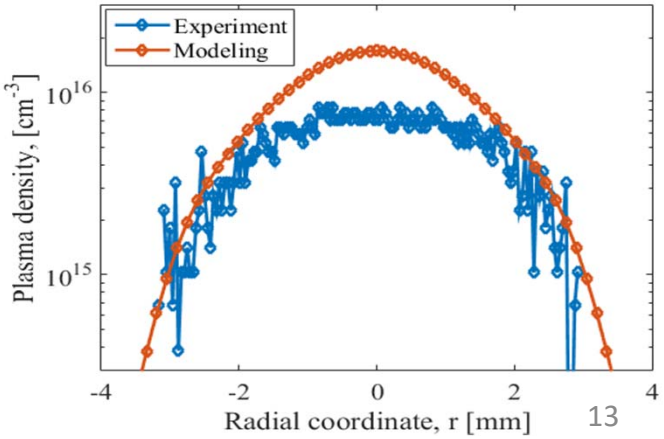

Gas flow controls transport of carbon in the arc

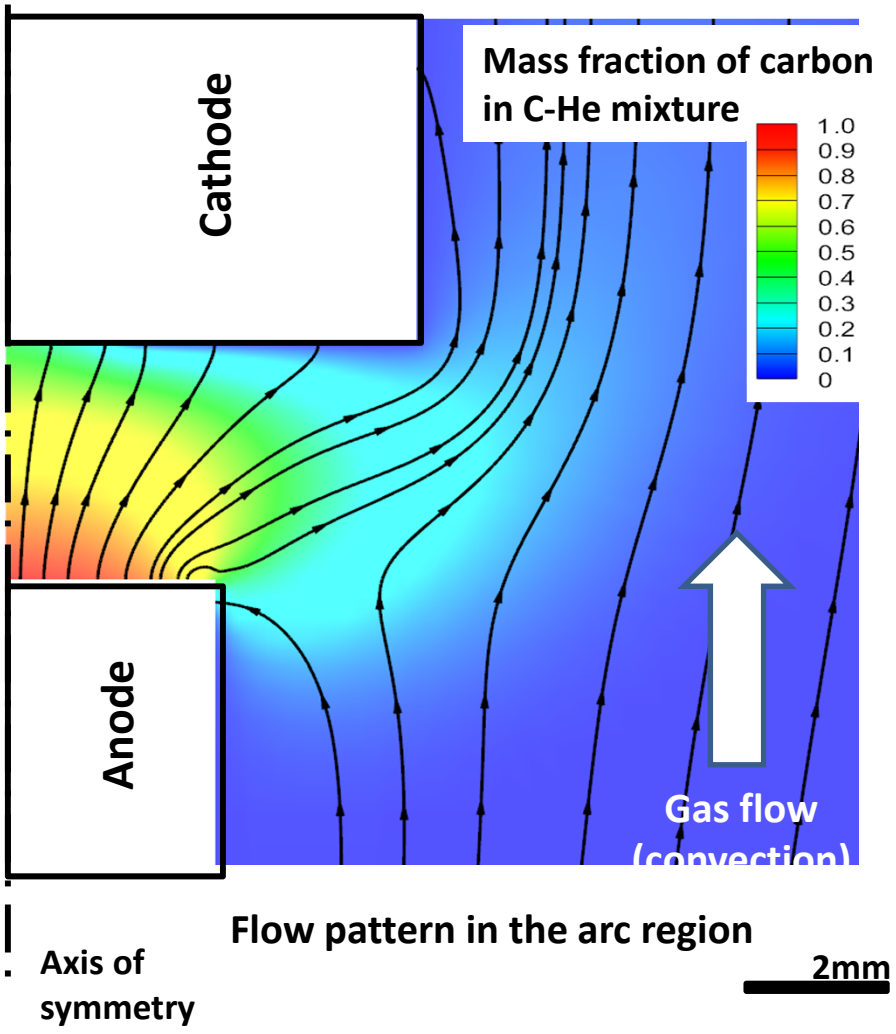

Flow pattern in the arc region

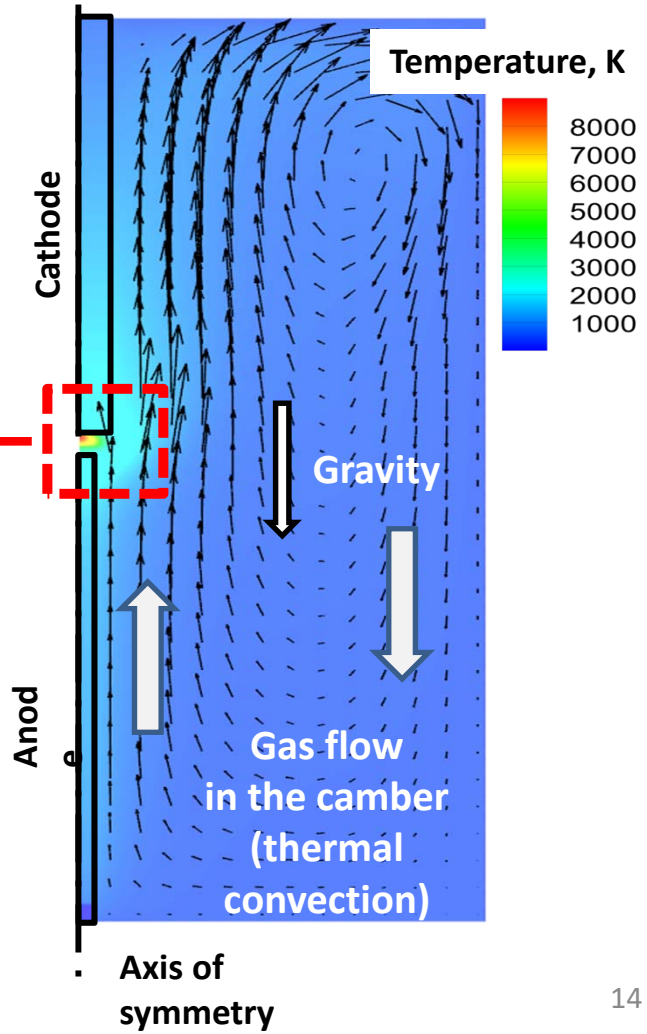

Unique in situ diagnostics of plasma synthesis

- Laser-Induced Fluorescence,
- Laser-induced incandescence,
- Coherent Rayleigh-Brillouin Scattering,
- Fast frame imaging,
- Fast extractor of nanoparticles,
- Ex-situ characterization of nanomaterials

Used Stark broadening effect to measure plasma density profiles

Used collisional radiative model to determine the electron temperature

Obtained spatial distribution of the carbon diatomic molecules by laser induced fluorescence (LIF) technique.

In-situ characterization of plasma and nanoparticles

Continuum Surelite III10

Laser-Induced Fluorescence
(LIF) to measure T and n of C_2, C_3, B, BH, etc.
Resolution: 10 ns, 100 µm

Laser-induced incandescence (LII) to detect nanoparticles of > 10's nm Resolution: 10 ns, mm's

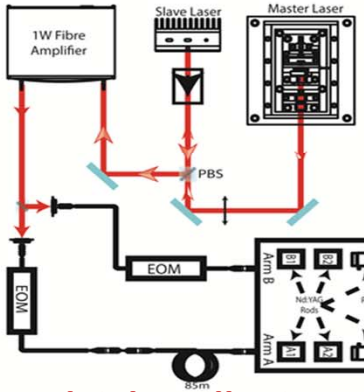

Coherent Rayleigh-Brillouin Scattering
(CRBS), to detect nanoparticles of 1-100 nm
Resolution: 10-1000 ns, 100 µm

Ex-situ characterization of nanomaterials by SEM, EDS, TEM, Raman spectroscopy, XRD, etc.

Optical emission spectroscopy, T_e, n_e, n_g

Fast frame imaging

Fast probe/ extractor of nanoparticles for ex-situ analysis

Arc chamber

CRBS – unique in-situ diagnostic of nanoparticles in volume

- **CRBS concept**

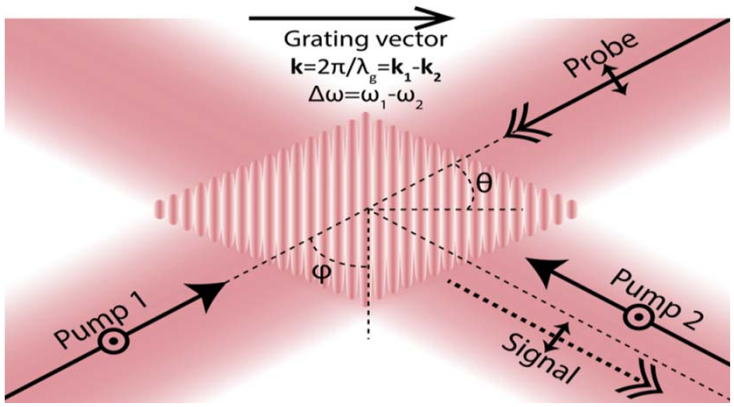

- **Detected signal in carbon arc**

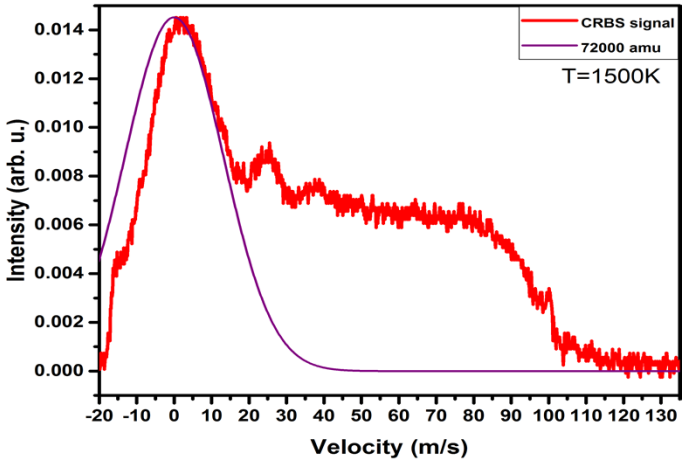

- **Two beams form optical lattice by ponderomotive force to produce coherent scattered signal, $I_{signal} \propto (\alpha \Delta N)^2$**
- **Measures nanoparticle relative concentrations, ΔN, temperature or mass, and flow velocity**
- **Detection limits depend on densities and polarizabilities of gas and nanoparticles, α.**
- **CRBS setup**

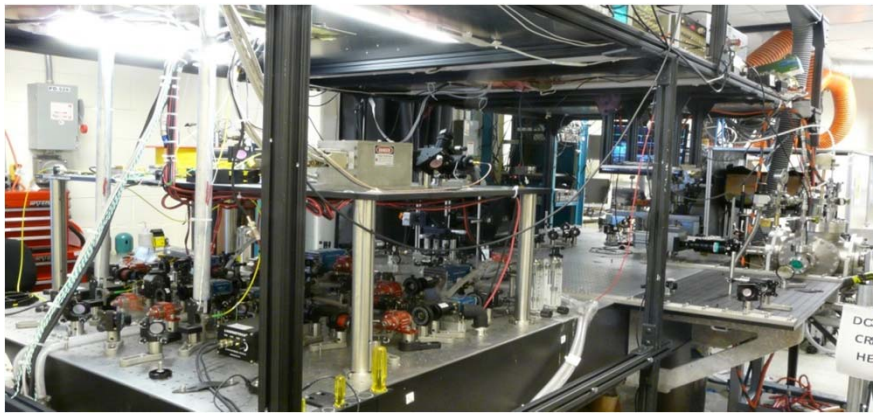

Complex structure of the carbon arc discharge for synthesis of carbon nanotubes

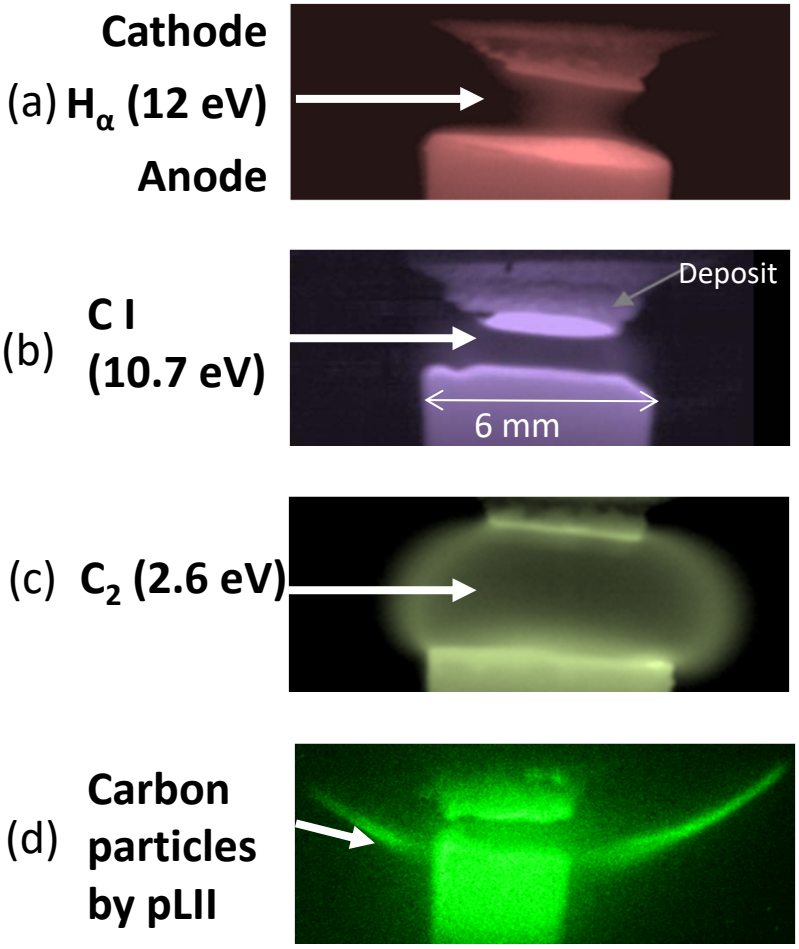

Emission measurements revealed different arc regions where evaporation (a,b), nucleation and growth of nanoparticles (c,d) occur. Hot arc core is populated mainly with carbon atoms and ions (a,b) and colder arc periphery (c) is populated mainly with C_2 , C_3 and far periphery (d) with arc generated nanoparticles:

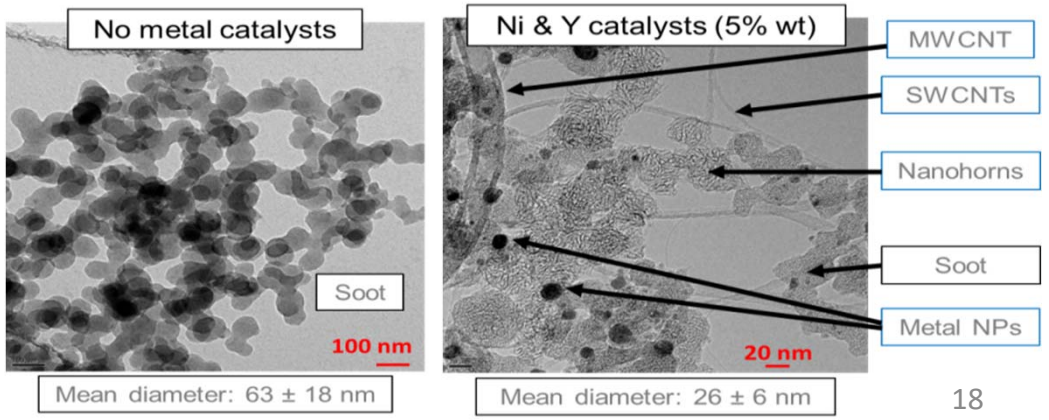

Towards predictive modeling of atmospheric plasma for synthesis of nanomaterials

- **Plasma density obtained from H_α OES and 2-D CFD simulations**

Arc operation: Current 55 A, He pressure 500 torr

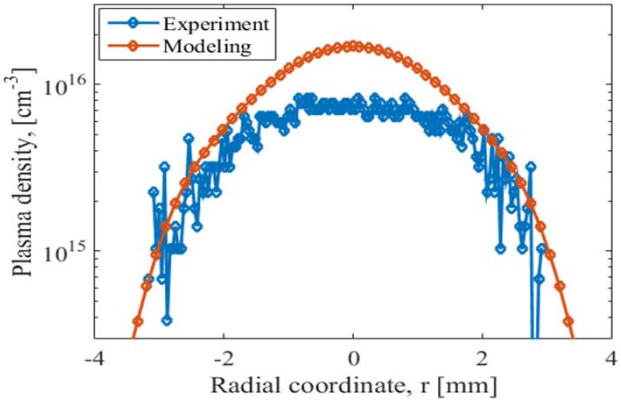

Inhomogeneity of the arc plasma is due to narrow arc channel

- **C_2 density obtained from LIF (a) and 2-D CFD (b)**

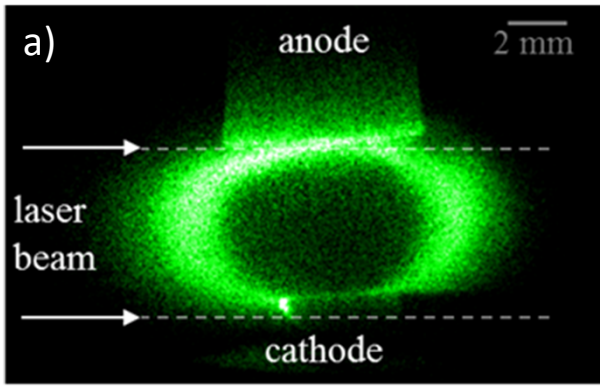

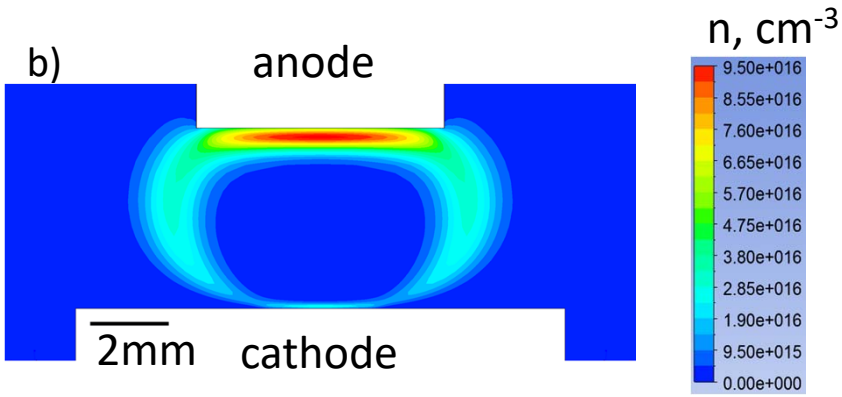

Summary of key results of measurements

Different regions: 1 – Evaporation 2 – Nucleation 3 – Growth

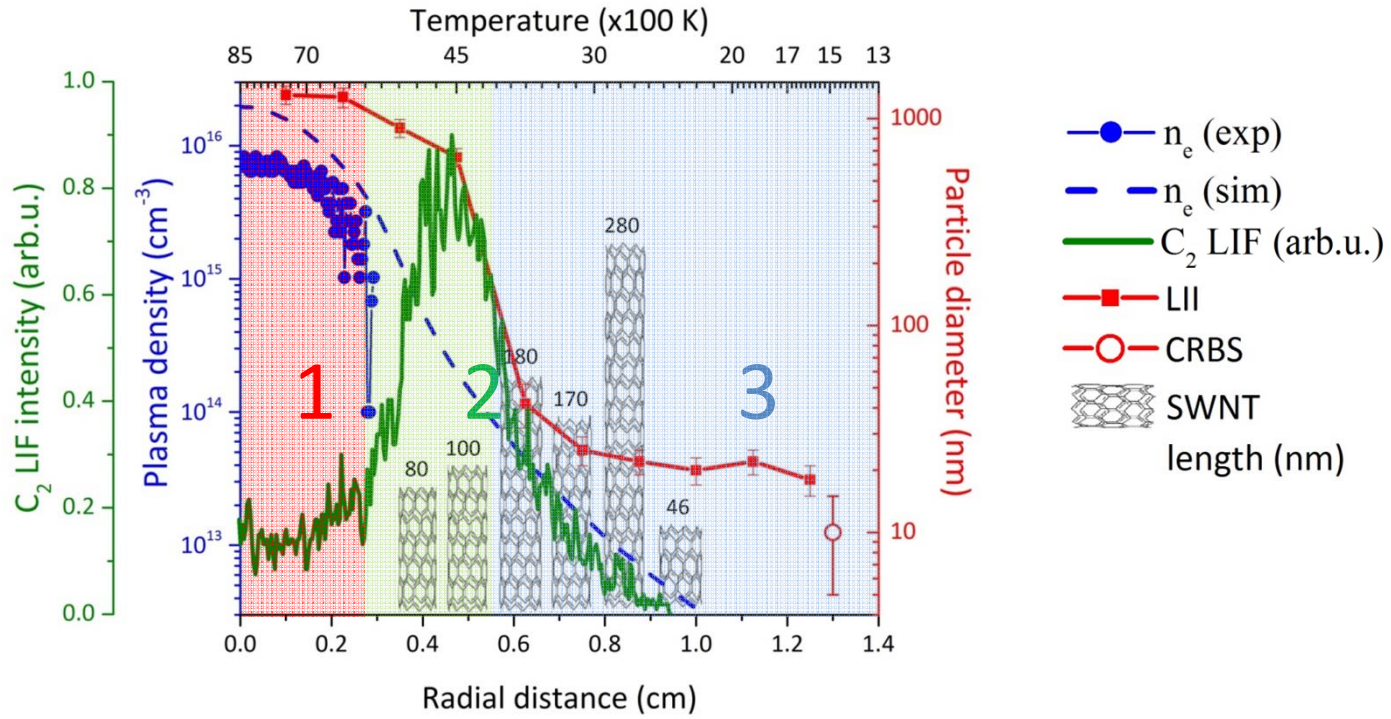

- **Arc current flows in the arc core (1). C_2 reaches maximum in region (2)**
- **CNTs are formed in non-equilibrium, colder plasma at the arc periphery (3)**
- **Carbon particles observed: in the core (1) ~ 1 µm, at periphery ~20 nm**

Measurements and simulations of nanoparticles

Experimental set up for laser-induced incandesce (LII), spectral imaging, and the laser beam intersection with the region of nanoparticle growth.

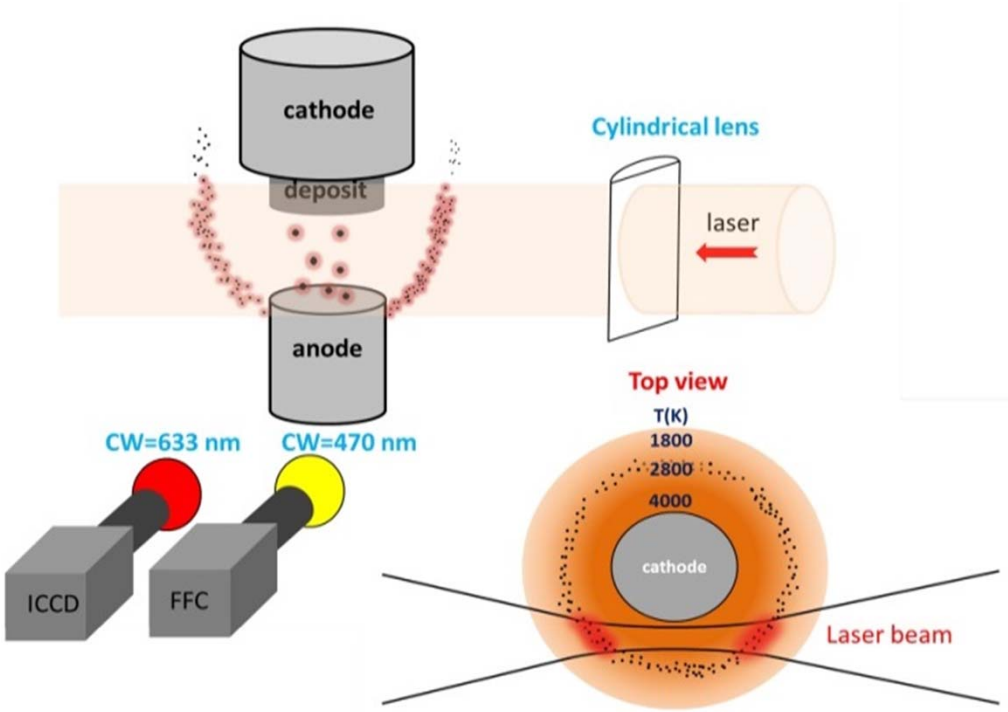

Areas from which a LII signal was collected are highlighted and the mean particle diameter for each area is shown from LII (yellow) and simulations (white). S. Yatom, et al, MRS (Material Research Society) Communications.

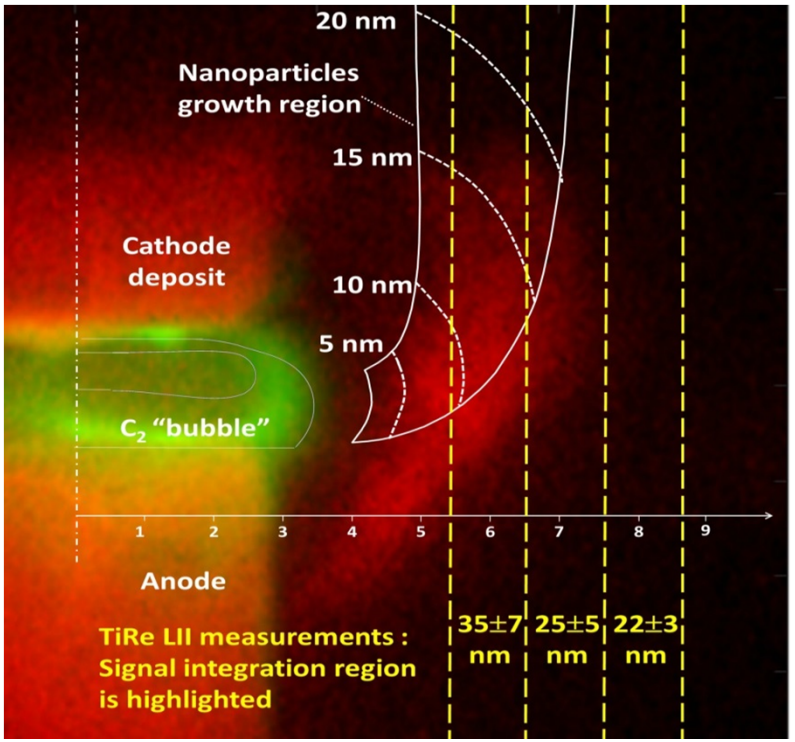

Outline

- **Atomistic simulations of key processes of nanotube growth**

Charging of SWCNTs could help in their growth

a)

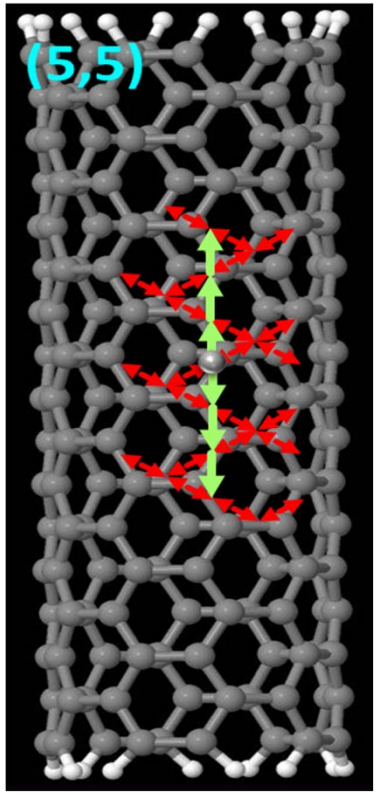

- **Charging of nanoparticles and nanostructures is a plasma effect on nucleation and growth processes**
- **DFT and Kinetic Monte-Carlo simulations of charging effect**
- **Armchair (5,5) SWCNT (Fig. a)**
- **Charging of the CNT causes the higher adsorption energy E_a, increasing the migration distance, (Fig. c)**

b)

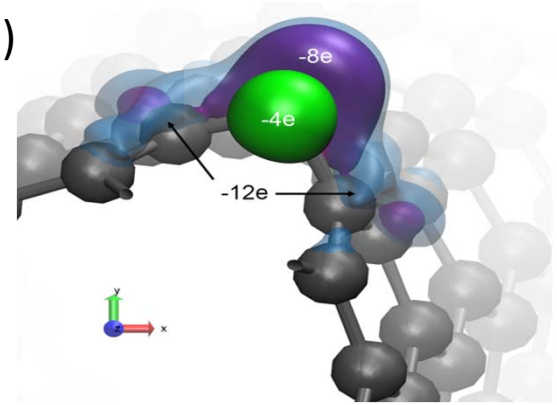

c)

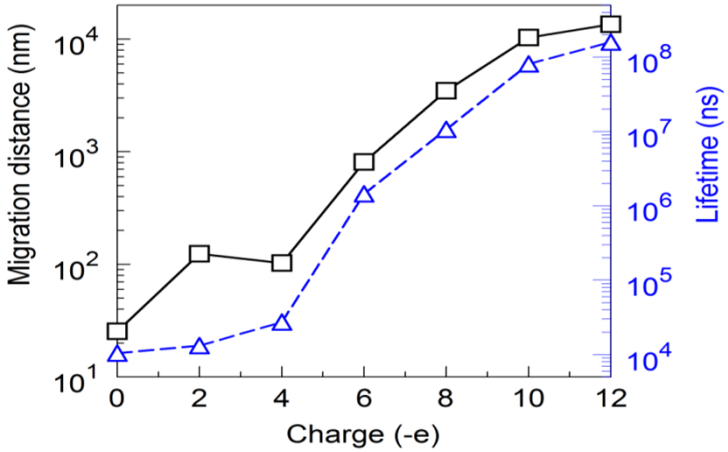

DFT results (Fig. b)- additional charges distribute in the covalent bond space between adatom and CNT, increasing its covalent coupling

Understanding of synthesis processes and synthesis selectivity of carbon nanotubes in arc

- **DFT simulations identified absorption energy and barriers for diffusion along the CNT surface.**
- **Analytical calculations and kinetic Monte Carlo method identified the rate of diffusion.**
- **Using carbon and dimer density profile the length of grown CNT can be determined**
- **It was found that it is function of chirality.**

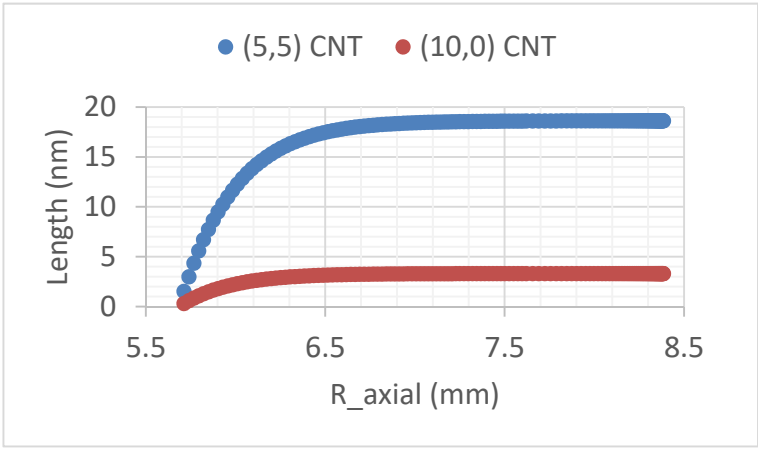

Binding Energy of C, C2 to CNT

5,5: T1 -3.21 -3.59; L1 -2.43 -2.66

10,0: T1 -2.59 -2.62; L1 -1.98 -2.64

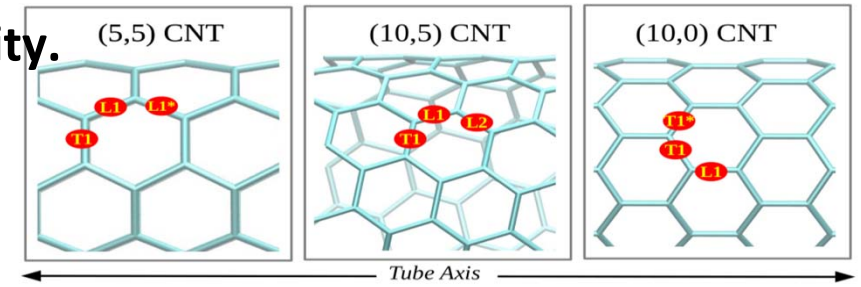

Average time and diffusion length before desorption

$$\langle t \rangle = \frac{2k_{12} + k_{21}}{2k_{12}k_{2d} + k_{21}k_{1d}}; \quad \mathrm{L} = \sqrt{2D\langle t \rangle}$$

Han, Kaganovich, Santra, et al., to be submitted

Understanding Root growth of BNNT

1. Accumulation of N on the surface of liquid boron
2. Formation of a BN island on the liquid surface
3. Fluctuation and nucleation of a protruding BN cap
4. Growth of the nanotube with root feeding

Order-parameter-driven molecular dynamics DFT simulations predicted formation of a BN cap at 2500 K, B. Santra et al. (2017)

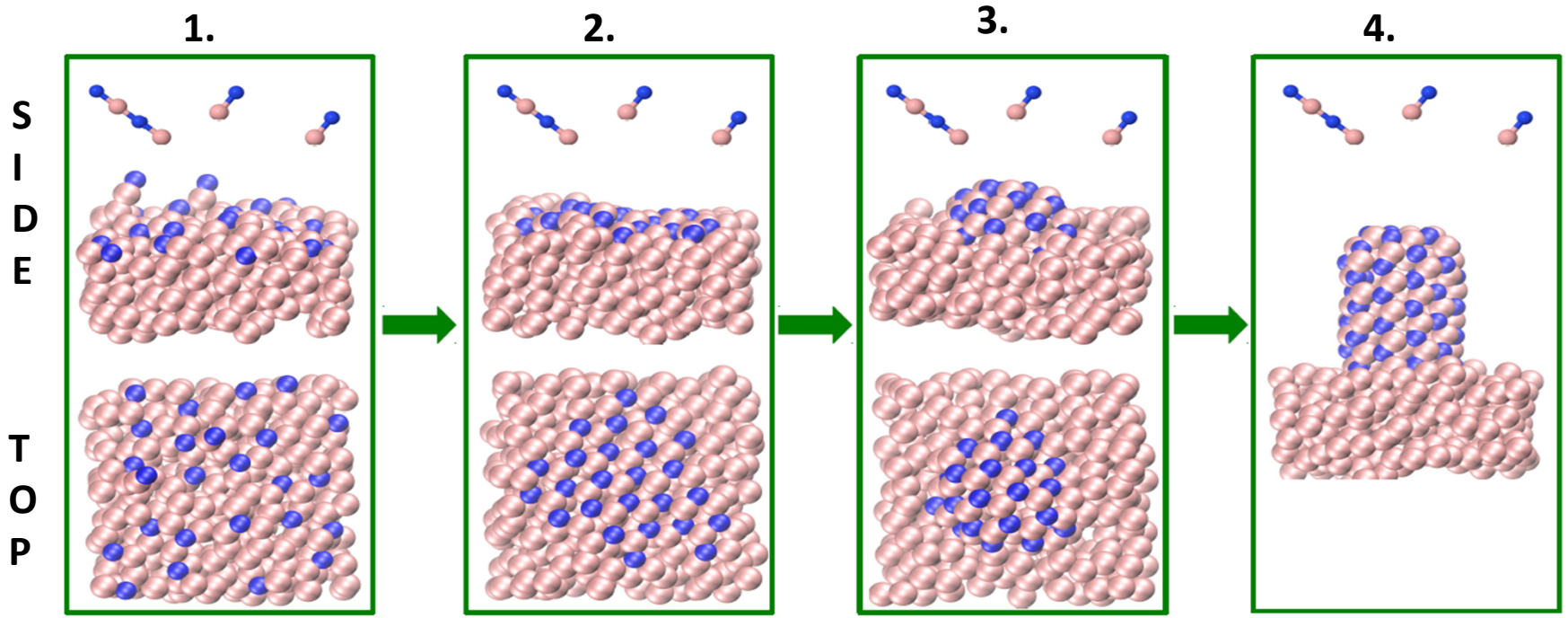

Encapsulation of boron particles

- **Simulations by Quantum-Classical Molecular Dynamics with Density Functional Tight Binding Theory**

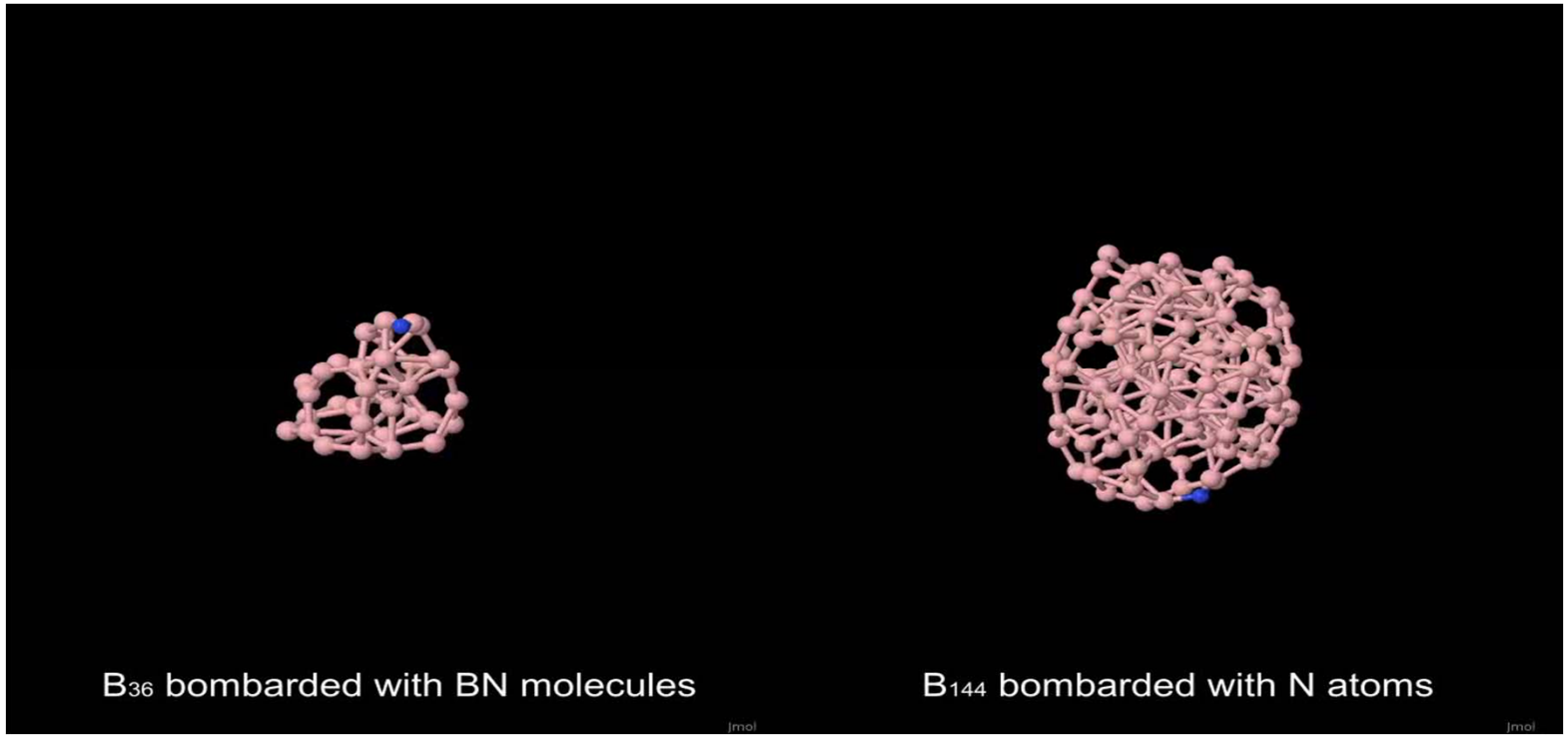

B-pink
N-blue

- **Bombardment by BN (left) or N (right) of boron cluster shows encapsulation of boron clusters with BN layers; the effect is observed in experiments by our and other groups**

P. Krstic et al., Chem. Sci. 9, 3803 (2018)

Outline

- **Nonstationary processes in arcs**

Observed two ablation modes affecting synthesis of carbon nanotubes

Low ablation

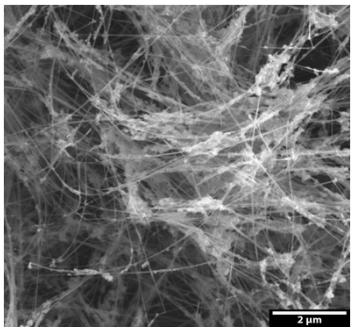

MWCNTs on the deposit

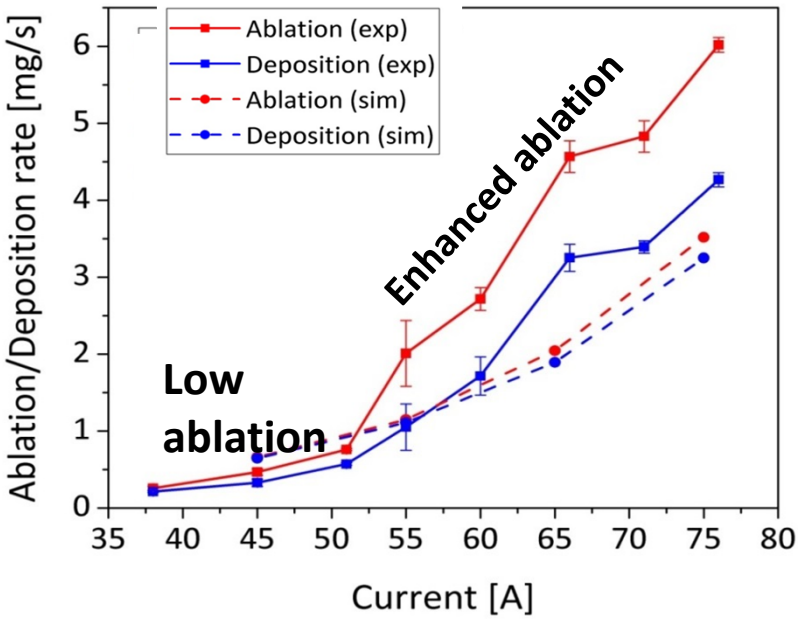

Enhanced ablation

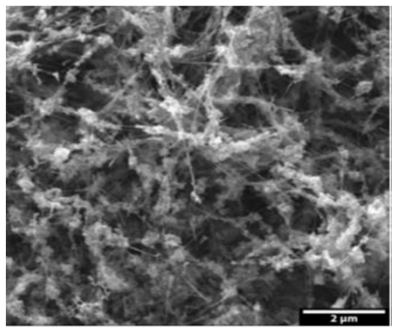

MWCNTs on the deposit

- **Correlation between synthesis selectivity, yield, arc geometry and current:**
  - **Enhanced ablation → Higher C_2 density → Deposition with higher yield**
  - **Smaller ablation → Reduced carbon flux → Deposition with better selectivity**

Arc oscillations affect synthesis of nanotubes

- **Synthesis of SWCNT by carbon arc with metal catalysts**
- **Metal – Carbon mixed powder filled in the hollow graphite anode rod**
- **Multi-mode oscillations: LF (10^2 Hz) and HF (10^3 Hz) modes, inside and outside the hollow anode**
- **Oscillations cause of low purity and poor selectivity of the arc synthesis**

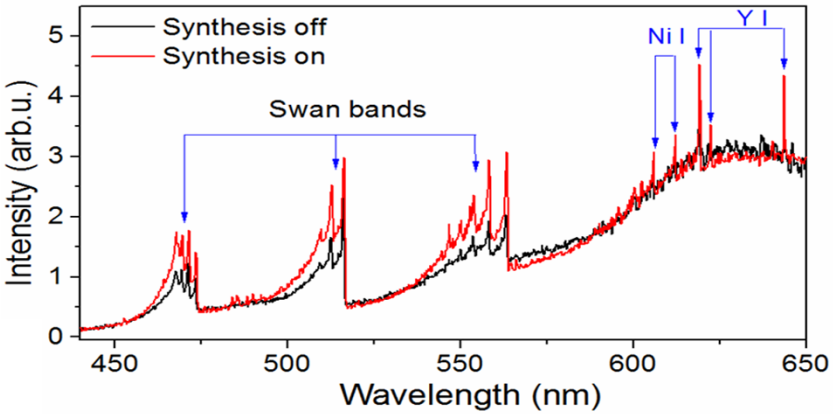

- **C_2 Filtered Fast Imaging, 10,000 fps**

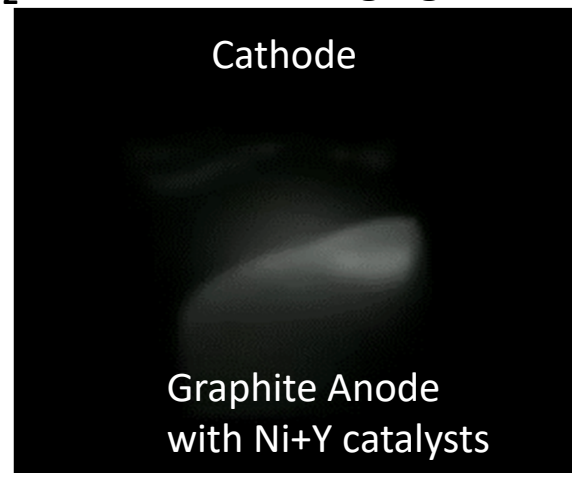

SWCNT Synthesis OFF

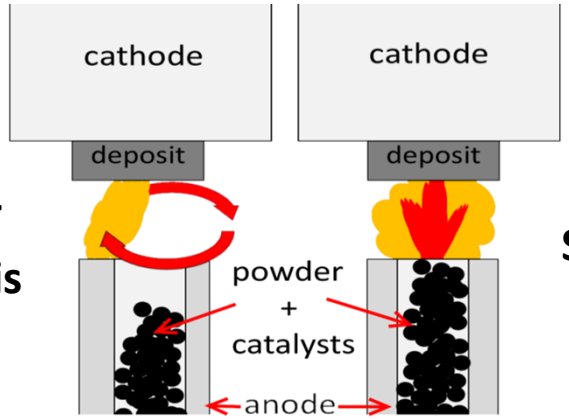

SWCNT Synthesis ON

~ 5% of time

Synthesis of BNNT by arc discharge

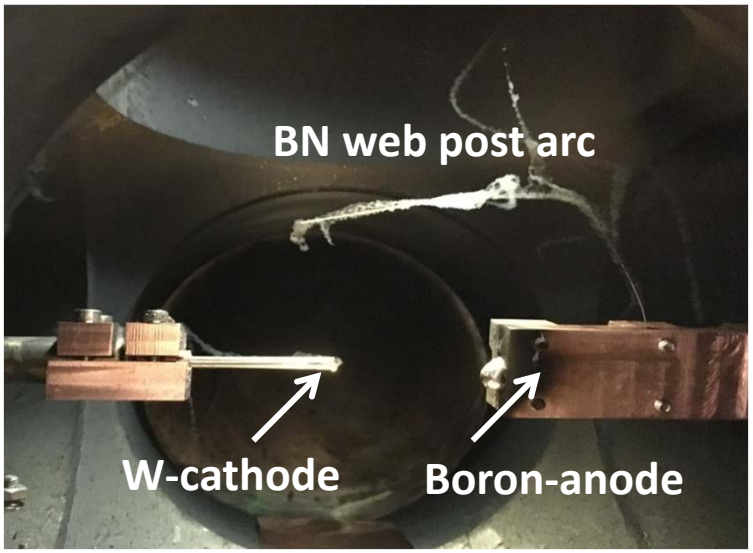

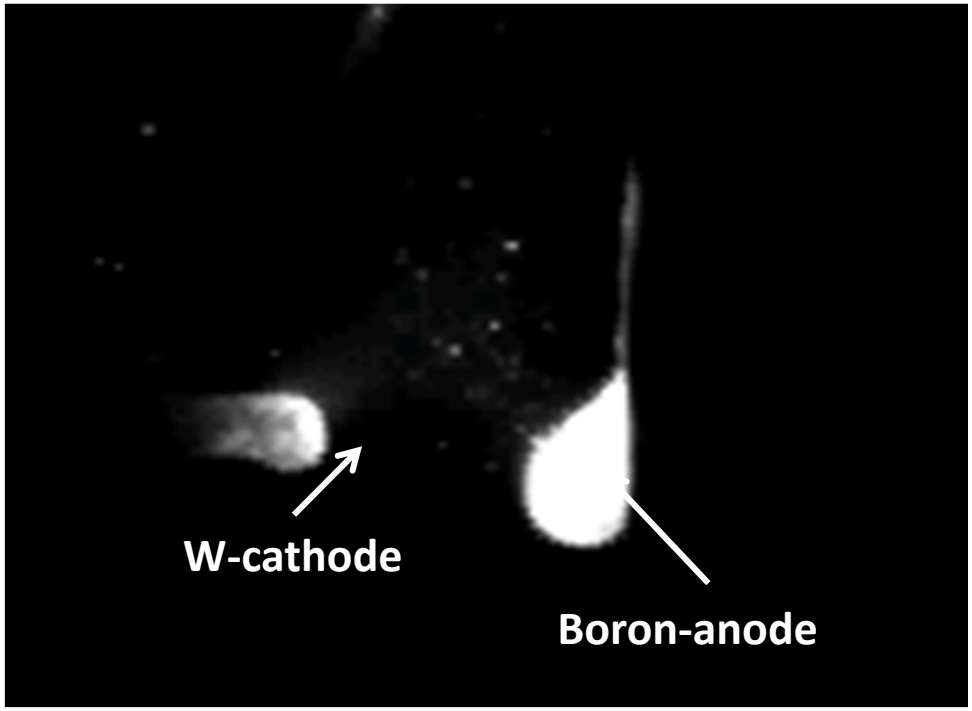

Boron-rich anode and tungsten cathde 40V-40A arc at 400 torr of N_2 (Zettl 2000)

Summary

- **All proposed in-situ diagnostics were developed and successfully applied to produce first comprehensive parametric characterization of arc plasma**
  - **Measured and modelled carbon species density, plasma temperature and particle distribution in arc.**
- **Fast frame imaging revealed arc oscillations (that have adverse affect on synthesis selectivity and purity of synthesized products).**